

Electric Supporting Information

Understanding Structure-Determining Solid Fluorescence of An Azaacene Derivative

*Pei-Yang Gu,^a Guangfeng Liu,^a Jun Zhao,^b Naoki Aratani,^c Xin Ye,^d Yang Liu,^d Hiroko Yamada,^c Lina Nie,^a Huanxiang Zhang,^e Jia Zhu,^e Dong-Sheng Li,^{*b} and Qichun Zhang^{*a,f}*

^aSchool of Materials Science and Engineering, Nanyang Technological University, Singapore 639798, Singapore.

*E-mail: qc Zhang@ntu.edu.sg

^bCollege of Materials and Chemical Engineering, Key Laboratory of Inorganic Nonmetallic Crystalline and Energy Conversion Materials, 443002, China

*E-mail: lidongsheng1@126.com

^cGraduate School of Materials Science, Nara Institute of Science and Technology, Ikoma, 630-0192, Japan

^dState Key Laboratory of Crystal Materials, Shandong University, Jinan, 250100, China

^eBeijing National Laboratory for Molecular Sciences (BNLMS), Institute of chemistry, Chinese Academy of Sciences, Beijing 100190, China.

^fDivision of Chemistry and Biological Chemistry, School of Physical and Mathematical Sciences, Nanyang Technological University, Singapore 637371, Singapore

Contents

Scheme S1. The structures of high emission molecules in solid states.

Figure S1. ^1H NMR spectrum of **TBIDQ**.

Figure S2. ^{13}C NMR spectrum of **TBIDQ**.

Figure S3. HR-MS of **TBIDQ**.

Figure S4. Normalized absorption and fluorescence emission spectra of **TBIDQ** in different dilute solutions.

Figure S5. Normalized emission of **TBIDQ** in hexane solution with different concentration.

Figure S6. Fluorescence decay of three polymorphs.

Figure S7. The ellipsoid plots of the three polymorphs.

Figure S8. The molecular stacking patterns and relative mean distances of interlayers of the three polymorphs.

Figure S9. 2D-finger print plots of the three polymorphs.

Figure S10. The short intermolecular interactions in the three polymorphs.

Figure S11. TGA curve of **TBIDQ**.

Figure S12. DFT molecular simulation result of **TBIDQ**: HOMO, LUMO and optimized geometrical structure.

Table S1. Crystallographic data and structure refinement parameters of three forms (CCDC number: 1526988 for Form I, 1526989 for Form II, 1526995 for Form III)

Experimental Section

Materials

cyclopenta[*fg*]acenaphthylene-1,2,5,6-tetraone, and 3,6-bis((triisopropylsilyl)ethynyl)benzene-1,2-diamine were synthesized according to the reported procedures.^{S1} Dichloromethane was distilled from calcium hydride. Tetrahydrofuran was distilled from sodium. Other chemicals and solvents were used directly without further purification.

Characterization

Using CDCl₃ as solvent and tetramethylsilane (TMS) as the internal standard, ¹H NMR and ¹³C NMR spectra were measured on a Bruker Advance 300 NMR spectrometer at ambient temperature. The UV-vis and fluorescence spectra in solutions were carried out on Shimadzu UV-2501 and RF-5301 spectrophotometer, respectively. High resolution mass spectrum (HRMS) was performed on a Waters Q-ToF premier mass spectrometer. The fluorescence decay times were performed on FS5 fluorescence spectrometer, Edinburgh Instruments Ltd..

Single-crystal X-ray diffraction. The suitable single-crystals were selected for single-crystal X-ray data collection with a Bruker SMART APEX-II CCD area detector on a D8 goniometer. The data were collected using graphite-monochromated and 0.5 mm-Mono Cap-collimated Mo-K α radiation ($\lambda = 0.71073 \text{ \AA}$) with the ω scan method at room temperature (Form I and Form II) and 100 K (Form III). The data were processed with the SAINT program of the APEX2 software^{S2} for reduction and cell

refinement. Multi-scan absorption corrections were applied by using the SADABS program for area detector. All structures were solved by the direct method and refined by the full-matrix least-squares method on F^2 .^{s3} All non-H atoms were refined anisotropically. Hydrogen atoms were placed in idealized positions and included as riding with Uiso (H) = 1.2 Ueq (C). Crystallographic data and structural refinements are summarized in Table S1.

The fluorescent quantum yields in dilute solutions were determined using quinine bisulfate ($\phi=54.6\%$ in 0.1 N H₂SO₄) as a standard using the equation:

$$\phi_s = \frac{F_s n_s^2 A_r}{F_r n_r^2 A_s} \phi_r \quad (1)$$

In this equation, subscripts s and r represent the sample and reference, respectively. F is the integral area of the fluorescence spectra, n is the refractive index of the solution, A is the absorbance, ϕ is the fluorescence quantum yield. Photoluminescence spectra (PL) and fluorescence quantum yield for single crystals were collected on an Edinburgh Instruments FLS 980 system spectrofluorimeter equipped with Xe-900 and integrating sphere.

Fluorescence microscope measurement. Fluorescence image was obtained using a Nikon Ti-U Inverted Microscope System equipped with a Nikon C-SHG 1 mercury lamp. The exposure time to acquire a bright photo on a fluorescence microscope is 60 ms with four attenuators (1/4, 1/8, 1/16, and 1/32).

Hirshfeld Surface Analysis

The Hirshfeld surfaces were generated using CrystalExplorer 3.1,^{s4} which imports a structure input file in the CIF format. In CrystalExplorer, bond lengths to hydrogen

atoms were normalized to typical neutron values (C-H = 1.083 Å).^{s5} The normalized contact distance (d_{norm}) based on d_e (the distance from the point on the surface to the nearest nucleus external to the surface) and d_i (the distance from the point on the surface to the nearest nucleus internal to the surface) and van der Waals radii of the atom are given by

$$d_{norm} = \frac{d_i - r_i^{vdw}}{r_i^{vdw}} + \frac{d_e - r_e^{vdw}}{r_e^{vdw}}$$

where r_i^{vdw} and r_e^{vdw} are the van der Waals radii of the atoms. The parameter d_{norm} is negative or positive, which is illustrated by a surface with a red-white-blue colored graph. Red spots represent lengths shorter than the van der Waals distance, while white areas and blue regions reveal lengths around and longer than the van de Waals distance, respectively.

Synthesis

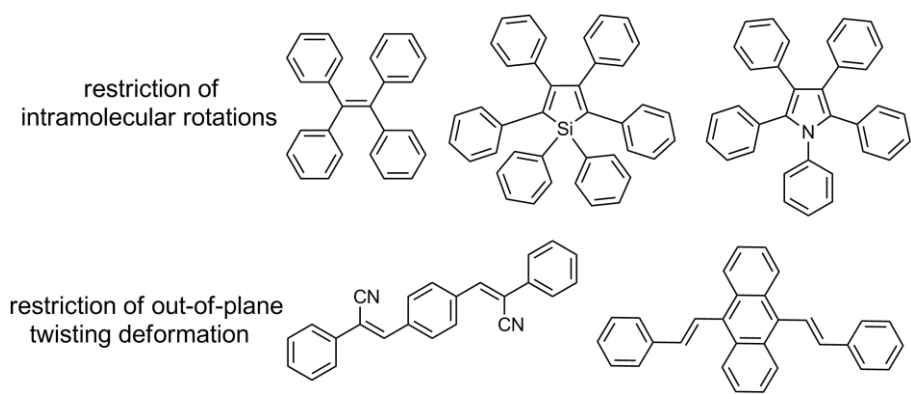
Synthesis of 1,4,9,12-tetrakis((triisopropylsilyl)ethynyl)benzo[1,8]-as-indaceno[2,3-*b*:6,7-*b'*] diquinoxaline (**TBIDQ**)

A mixture of 3,6-bis((triisopropylsilyl)ethynyl)benzene-1,2-diamine (103 mg, 0.22 mmol) and cyclopenta[*fg*]acenaphthylene-1,2,5,6-tetraone (23.6 mg, 0.1 mmol) in acetic acid (20 mL) was stirred and heated to 118°C under nitrogen for 48 h. After cooling to room temperature, the mixture was poured into water and the crude product was purified by column chromatography over silica gel, eluting with DCM/hexane to give **TBIDQ** (84 mg, 0.077 mmol, 77%).

¹H NMR (300 MHz, CDCl₃) δ 8.35 (s, 4H), 7.85 (s, 4H), 1.32 (s, 84H).

¹³C NMR (75 MHz, CDCl₃) δ 156.46, 142.00, 134.90, 134.55, 133.28, 124.74, 124.61, 103.54, 100.14, 18.87, 11.55.

HR-MS, formula, C₇₀H₉₃N₄Si₄; Calc. mass, 1101.6472; found, 1101.6432.



Scheme S1. The structures of high emission molecules in solid states.

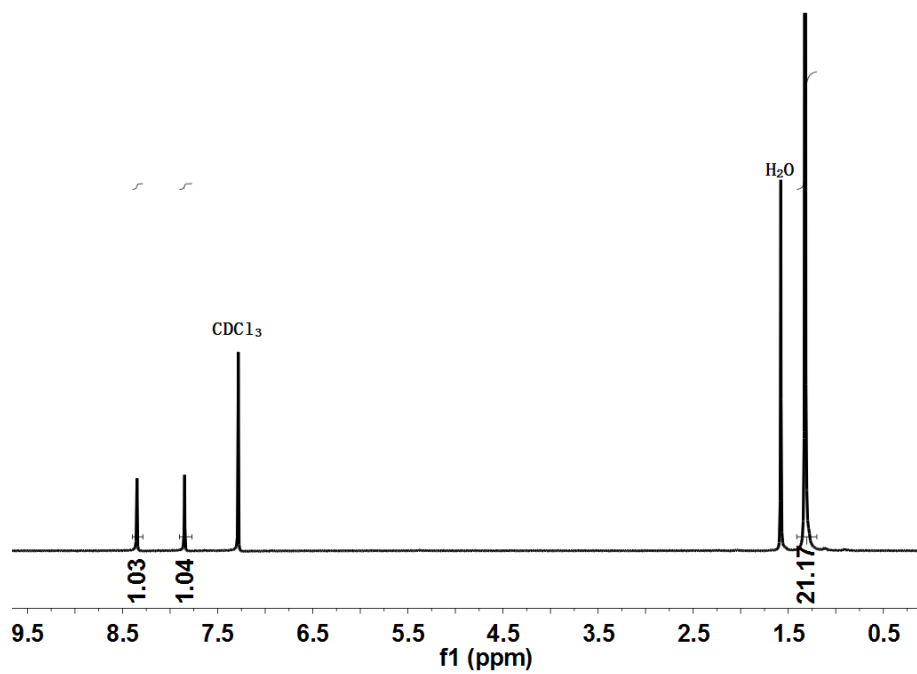


Figure S1. ^1H NMR spectrum of **TBIDQ**.

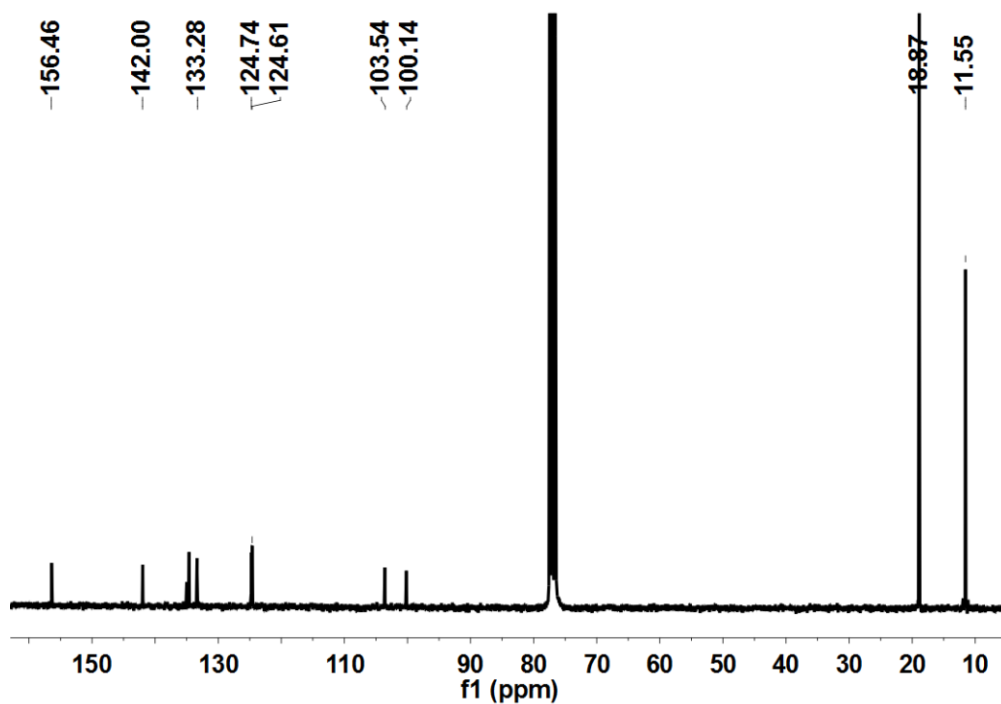


Figure S2. ^{13}C NMR spectrum of **TBIDQ**.

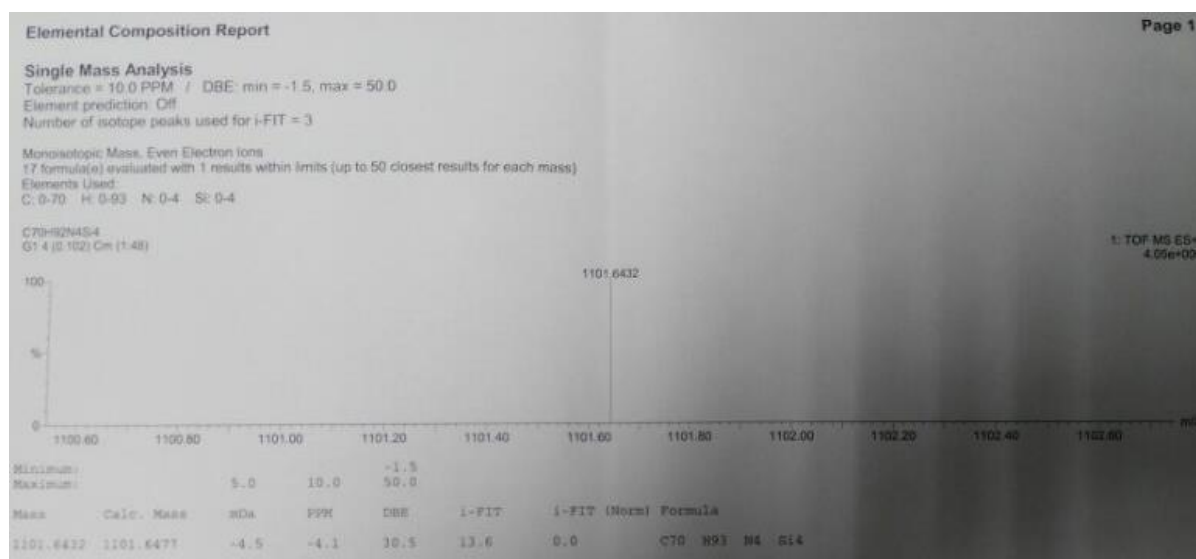


Figure S3. HR-MS of **TBIDQ**.

The shoulder peak might originate from the molecular aggregation because the solubility of **TBIDQ** in hexane is poor. Note that the shoulder peak disappears by changing the solvents from hexane (poor solvent) to toluene, chloroform, or THF (good solvents, **Figure S4b**), further confirming that the shoulder peak emission is

caused by aggregated states. Furthermore, the normalized emission spectra of different concentrations of TBIDQ in hexane have been provided in **Figure S5**. The photoluminescence (PL) intensity at 545 nm is decreased with increasing the concentration of TBIDQ in hexane.

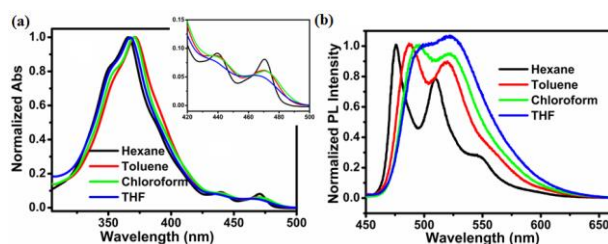


Figure S4. Normalized absorption and fluorescence emission spectra of **TBIDQ** in different dilute solutions.

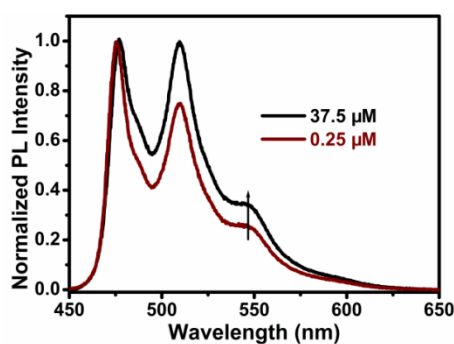


Figure S5. Normalized emission of **TBIDQ** in hexane solution with different concentration.

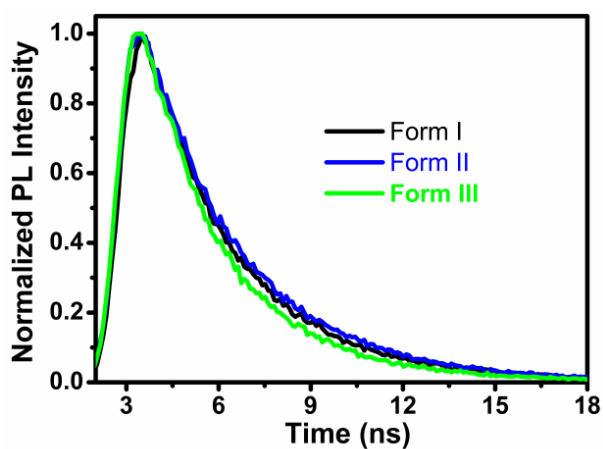


Figure S6. Fluorescence decay of three polymorphs.

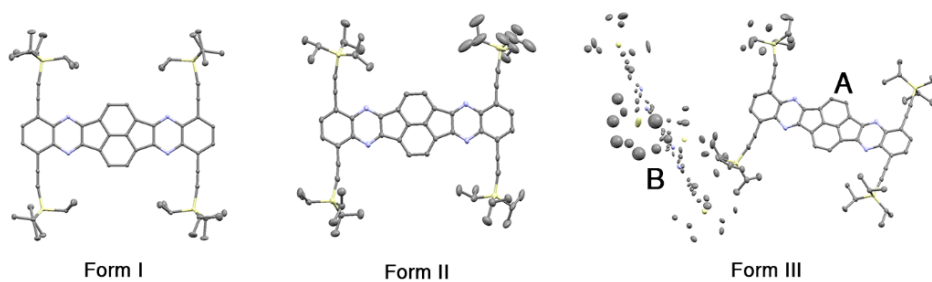


Figure S7. The ellipsoid plots of the three polymorphs. The part A molecule is more ordered than the part B molecule in Form III. (50% probability ellipsoid, color scheme: C, grey; N, blue; Si pale yellow. H atoms are omitted for clarity).

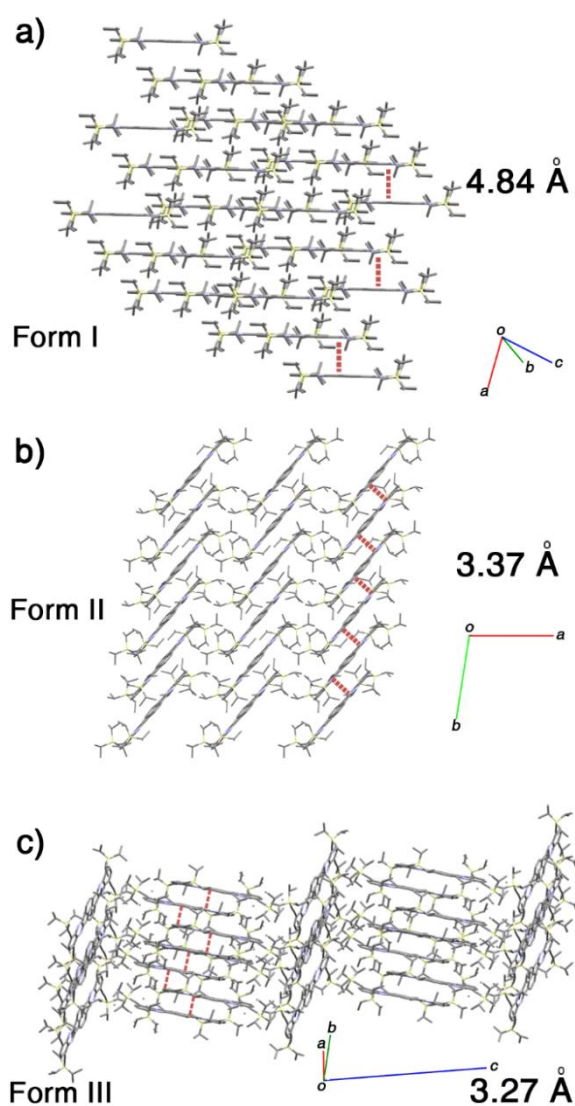


Figure S8. The molecular stacking patterns and relative mean distances of interlayers of the three polymorphs

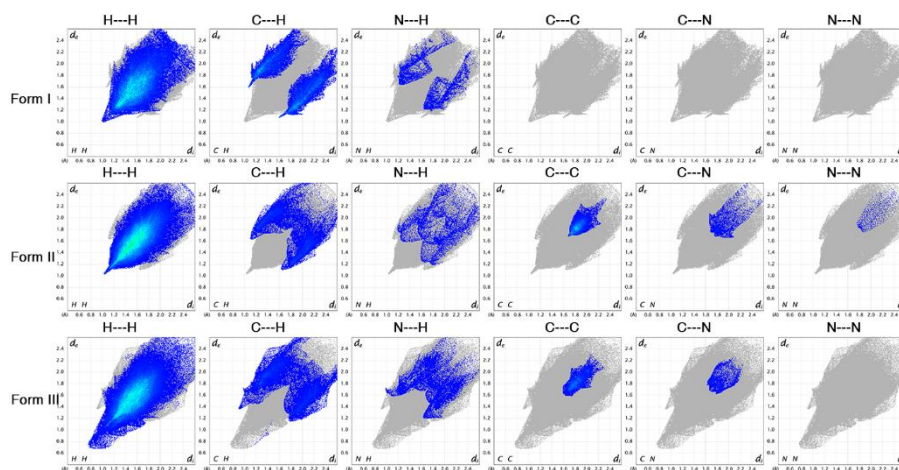


Figure S9. 2D-fingerprint plots of the three polymorphs

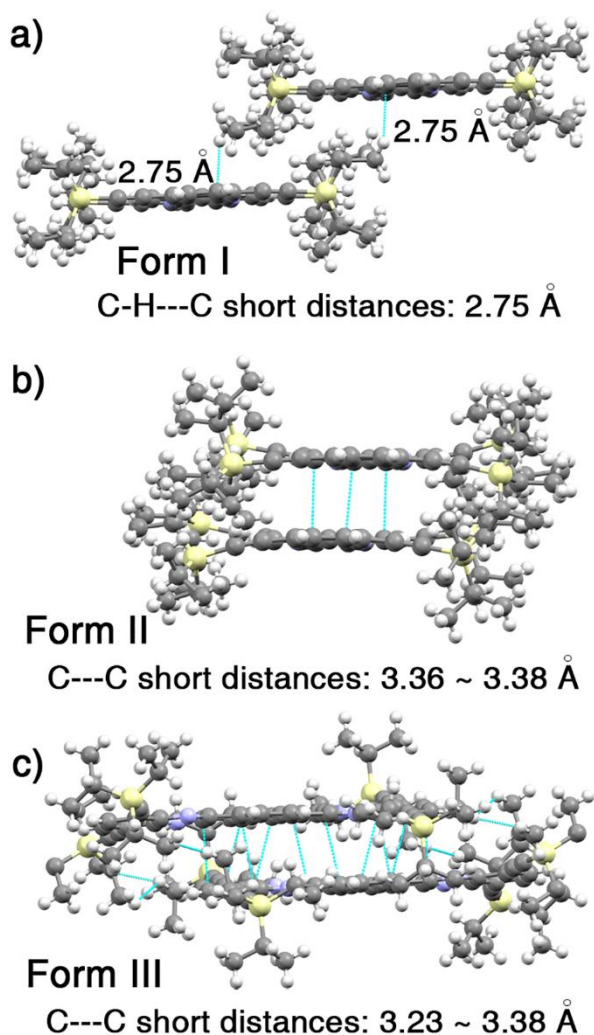


Figure S10. The short intermolecular interactions in the three polymorphs

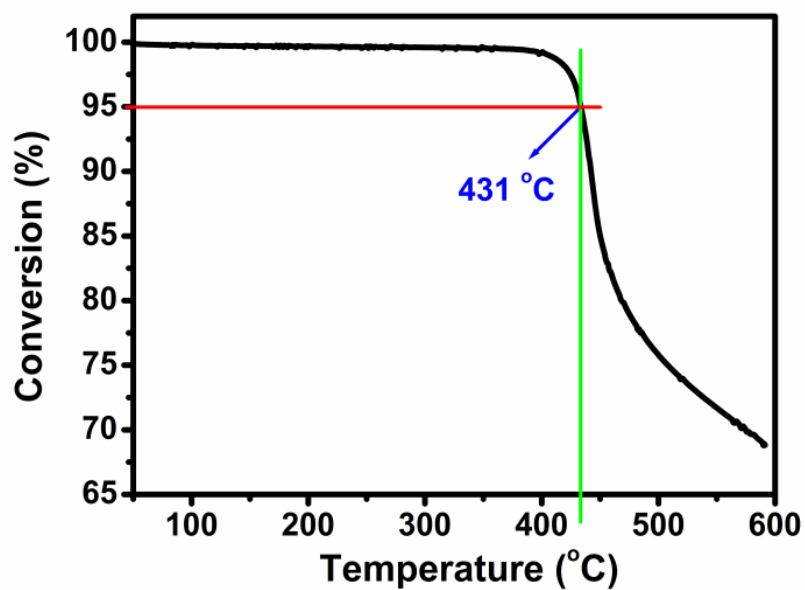


Figure S11. TGA curve of TBIDQ.

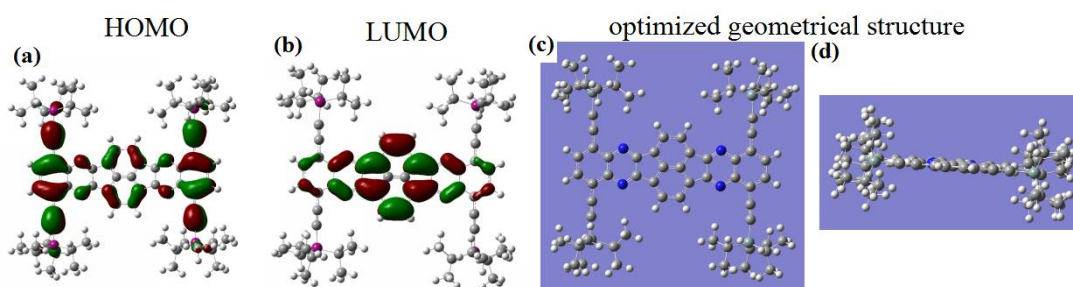


Figure S12. DFT molecular simulation result of TBIDQ: HOMO, LUMO and optimized geometrical structure.

Table S1 Crystallographic data and structure refinement parameters of three forms

(CCDC number: 1526988 for Form I, 1526989 for Form II, 1526995 for Form III)

	Form I	Form II	Form III
<i>T</i> (K)	296 (2)	296 (2)	103 (2)
Formula	C70 H92 N4 Si4	C70 H92 N4 Si4	C70 H92 N4 Si4
Formula weight	1101.84	1101.84	1101.84
Crystal system	triclinic	triclinic	triclinic
Space group	$P\bar{1}$	$P\bar{1}$	$P\bar{1}$
Z	1	2	3
<i>a</i> (Å)	11.423 (3)	13.810 (4)	7.7046 (2)
<i>b</i> (Å)	11.567 (3)	14.307 (4)	18.0195 (5)
<i>c</i> (Å)	13.150 (3)	18.434 (6)	35.6738 (9)
α (deg)	86.245 (2)	108.659 (3)	84.611 (6)
β (deg)	79.518 (2)	106.439 (3)	85.683 (6)
γ (deg)	72.596 (2)	92.843 (3)	82.538 (6)
<i>V</i> (Å³)	1630.2 (7)	3270.0 (17)	4879.1 (2)
ρ calcd (g/cm³)	1.122	1.119	1.125
λ (Mo Kα) (Å)	0.71073	0.71073	0.71073
Collected reflns	19332	79636	59863
Unique reflns	7425	15343	15304
Parameters	536	727	1374
<i>R</i> (int)	0.0138	0.0964	0.1104

R₁ [$I > 2\sigma(I)$]	0.0301	0.0903	0.0716
wR₂ [$I > 2\sigma(I)$]	0.0872	0.2359	0.1462
GOF	1.042	1.060	1.034

Reference

- S1. a) L. Zhu, Z. S. Fu, H. J. Pan, W. Feng, C. Chen and Z. Q. Fan, *Dalton Trans.*, 2014, **43**, 2900–2906; b) P. Biegger, S. Stolz, S. N. Intorp, Y. Zhang, J. U. Engelhart, F. Rominger, K. I. Hardcastle, U. Lemmer, X. Qian, M. Hamburger and U. H. Bunz, *J. Org. Chem.*, 2015, **80**, 582–589; c) B. D. Lindner, J. U. Engelhart, O. Tverskoy, A. L. Appleton, F. Rominger, A. Peters, H. J. Himmel and U. H. Bunz, *Angew. Chem. Int. Ed.*, 2011, **50**, 8588–8591.
- S2. APEX2 (version 2009.9-0); Bruker AXS Inc., Madison, WI, 2009
- S3. G. M. Sheldrick, *Acta Crystallogr. Sect. A* **2008**, 64, 112–122.
- S4. a) M. A. Spackman, D. Jayatilaka, *CrystEngComm* **2009**, 11, 19–32; b) M. A. Spackman, J. J. Mckinnon, *CrystEngComm* **2002**, 4, 378–392; c) M. A. Spackman, J. J. Mckinnon, D. Jayatilaka, *CrystEngComm* **2008**, 10, 377–388.
- S5. F. H. Allen, D. G. Watson, L. Brammer, A. G. Orpen, R. Taylor, *International Tables for X-ray Crystallography, Vol. C*, Kluwer Academic Publishers, Amsterdam, **2006**, Chap. 9.5, pp. 790–811